 CMC, vol.4, no.1, pp.31-42, 2006

Microstructure Optimization in Fuel Cell Electrodes using Materials Design

Dongsheng Li[1,2], Ghazal Saheli[1], Moe Khaleel[2] and Hamid Garmestani[1]

Abstract: A multiscale model based on statistical continuum mechanics is proposed to predict the mechanical and electrical properties of heterogeneous porous media. This model is applied within the framework of microstructure sensitive design (MSD) to guide the design of the microstructure in porous lanthanum strontium manganite (LSM) fuel cell electrode. To satisfy the property requirement and compatibility, porosity and its distribution can be adjusted under the guidance of MSD to achieve optimized microstructure.

keyword: Materials design, Fuel cell, Electrode, Statistical mechanics, Multiscale.

1 Introduction

With the emergence of a new possible energy crisis, last decade saw a huge increase of research activity on fuel cell. Fuel cell is one of the most promising power generator systems because of its high efficiency, excellent environmentally friendly features, portability (for polymeric electrolyte fuel cell) and low noise. The first fuel cell was, built more than a century ago by Williams Grove (1839). Some fuel cell power generation systems scaled up to 250kW have been built and tested by Siemens Westing, one of the prominent players in this area [Williams, Strakey and Singhal (2004)]. Department of Energy, military agencies investment banks are all funding the development of fuel cell for different applications. For economic, geopolitical, social and environmental reasons, the current interest on fuel cell research will stay or even increase.

Nevertheless, fuel cells are still waiting in the wings. The biggest hurdle is the high initial cost. To make it economically feasible to replace other more common energy sources, there is strong demand to improve the materials used in fuel cell. A typical fuel cell is composed of ion conducting electrolyte yttria stabilized zirconia (YSZ), a ceramic composite anode comprised of YSZ and Ni, porous cathode lanthanum strontium manganites and interconnects alkali doped lanthanum chromite. In this work, we will concentrate on using microstructure sensitive design to guide the microstructure and properties optimization in electrodes. The same methodology can be applied in other materials used in fuels cells. Procedures of materials design for different component materials in fuel cells are based on different properties requirement.

To commercialize fuel cells in large scale, two major issues must be solved in electrodes. One is to fabricate uniform efficient electrode in large scale. The other one is to improve the performance by optimizing microstructure. To address the above two challenges, our laboratory focused on two areas of research: One is fabrication of gradient porous electrode materials using aerosol assisted chemical vapor deposition (AACVD) and spray pyrolysis (SP). The other is to achieve optimized microstructure with best performance by using Microstructure Sensitive Design (MSD) to guide experimental work. There are also some other issues not covered in this work, such as catalyst design and assembly design.

The electrodes (anode and cathode) are porous media. Hydrogen, oxygen and steam can only occupy the pore space of the electrode and transport through the channel. Porosities in both anodes and cathodes are typically 25-40%. O^{2-} ions can only diffuse through the electrolyte and electrons can only flow in the solid part of the electrodes. Thus, electrochemical reactions occur only at the triple-phase boundaries (TPB) where the electrolyte meets both the solid and the porous regions of the electrodes. Factors that facilitate the electrochemical reactions and contribute to the efficiency of fuel cells are: 1) the ability for hydrogen to easily diffuse through the electrodes and reach the TPB, 2) a large number of TPB (more precisely, the triple-phase boundaries should have large length) and 3) the solid part of the electrodes should be a good conductor of electricity. These three factors depend on the microstructure of the electrode and the shape of the electrode electrolyte boundary. In electrode

[1] School of Materials Science and Engineering, Georgia Institute of Technology, 771 Ferst Dr. Atlanta, GA 30332-0245

[2] Pacific Northwest National Laboratory, Richland, WA 99352, U.S.

supported fuel cells, mechanical properties of electrodes are also very important. Large elastic modulus is needed to minimize the deformation under stress due to external force or thermal expansion. To achieve maximum performance, one of the challenges is to find the microstructure that optimizes these properties and satisfies processing constraints.

In summary, important goals in electrode materials are high mixed conductivity, great permissibility, long term stability, large reaction area/length, desired electrocatalytic activity, good chemical and thermal expansion compatibility. These requirements sometimes conflict each other. For example, good transport properties require large porosity while high conductivity and elastic modulus means low porosity. To satisfy these somehow incompatible criteria, gradient porous microstructure is a solution [Zhu and Deevi (2003)]. The layer close to the surface of the electrolyte is expected to be fine and the outer layer is coarse. Previous research works on multilayer electrodes showed better overall performance. By changing the percentage of porosity, pore size, and its distribution, both concentration and activation polarizations were minimized. When multiplayer is introduced, another issue should be taken into consideration: compatibility of properties in different layers. Similar topic in the compatibility (including chemical reactivity, thermal expansion) has been under intensive research.

Porous media can be considered to belong to a larger class of heterogeneous materials which includes composites (solids formed by two or more pure solid phases) and polycrystalline materials. A large number of mathematical methods have been developed to predict the properties of heterogeneous materials [Shen and Atluri (2004)]. These include analytical methods that provide estimates or bounds on the material properties [Castaneda (1991); Walpole (1981); Willis (1981)], numerical methods [Rodin (1993); Greengard and Moura (1994); Michel, Moulienec and Suquet (2001)] and methods based on the theory of percolation [Gavarri, Tortet and Musso (1999)].

Most analytical methods share the common feature of being computationally efficient and in many cases they provide explicit formulae in terms of properties of the pure phases (i.e. conductivity, etc.) and some characteristics of the microstructure (such as volume fraction of each pure phase). However, their accuracy becomes uncertain in the high contrast regime, i.e. when the properties of the phases are very different. This is certainly the case of porous media. For example, in a metallic porous media filled with gas, the electrical conductivity of the solid metal is many orders of magnitude higher than the conductivity of the gas that fills the pores.

On the other hand, the numerical methods cited above compute in the microscopic fields and obtain the macroscopic properties. The advantage of this approach is that it provides exact results (up to numerical errors). However, their computational cost becomes prohibitively expensive in the high contrast regime. Percolation methods do provide analytical expressions for the transport properties in the high contrast regime and thus are applicable to porous media. However, it can only be applied to a restricted class of microstructures. Asymptotic expansions in the high contrast regime have been developed for composites [Torquato (2002)]. However, they cannot be directly applied to porous media.

In this work, MSD is used to guide the microstructure optimization of electrodes. MSD comprises a mathematical framework for a rigorous treatment of microstructure as a design variable in highly-constrained design problems (Fig. 1). It has been developed to address the central inverse problem of materials design, that is to say, how to proceed from the stipulated objectives and constraints of the designer, to the specification of material microstructure predicted to meet these requirements [Adams et.al. (2001, 2004), Li and Garmestani (2003, 2005), Kalidindi et.al. (2004)]. In electrode materials, we concentrate on how to identify a certain porous gradient microstructure and material from a given set of properties (transport, mechanical, electrical, chemical stability, thermal expansion . . .).

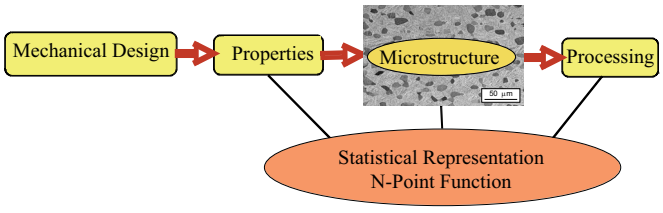

Figure 1 : Microstructure Sensitive Design flow chart

A multiscale model based on statistical continuum mechanics was used in this MSD to predict the electrical and mechanical properties of porous electrodes. The advantage of statistical mechanics over numerical methods such as finite element methods is the computational effi-

ciency. By using the statistical formula to characterize the microstructure in electrodes, the computation time shrinks in orders.

The rest of the paper is as follows: Section 2 is on statistical formula to characterize microstructure in heterogeneous materials. We present the multiscale model in Section 3 to predict mechanical and electrical properties in porous electrodes. Application of this multiscale model in microstructure sensitive design to guide the materials design of multi functional electrodes is discussed in Section 4. We close in Section 5 with final remarks.

2 Representation of Microstructure by Correlation Functions

The statistical details of a heterogeneous media can be represented by an n-point probability distribution function [Garmestani and Lin (2000 and 2001); Lin, Garmestani and Adams (1998 and 2000)]. Volume fraction, commonly used to capture the complexity of a microstructure, is in fact a one-point probability distribution function. Consider the porous electrode in a fuel cell made of LSM as phase 1, and the void as phase 2. Let the sample occupy a subset of space $V \subset R^d (d = 3)$ that is partitioned into two disjoint phases: LSM V_1 and voids V_2 such that $V = V_1 \cup V_2$ and $V_1 \cap V_2 = \Phi$. An indicator function $L^i(x)$ for phase i is used to identify a random point x, located inside or outside of phase i:

$$L^i(x) = \begin{cases} 1, & x \in V_i \\ 0, & otherwise \end{cases} \tag{1}$$

By definition volume fraction for phase i, v_i, is considered a one-point correlation function

$$\phi_i = P\left\{L^i(x) = 1\right\} \tag{2}$$

It is clear that volume fraction alone cannot capture the whole complexity of morphology in random heterogeneous media when studying effective properties. One example is the difference observed when two bounding theories, series and parallel, are used respectively in the prediction of properties for a composite with the same volume fraction. More details of the shape and morphology of the microstructure including the interaction of the components in the media and orientation distribution of crystallographic grains (texture) should be considered in order to give a reasonable prediction of effective properties. This can only be realized by using higher order distribution functions [Kroner (1977); Corson (1974) and Torquato (2002)]. A two-point distribution function is defined as a conditional probability function when the statistics of a three-dimensional vector, $\vec{r} = \vec{r}_2 - \vec{r}_1$, is investigated once attached to each set of random points in a particular microstructure:

$$P_{i_1 i_2}(\vec{r}) = P\left\{L^{i_1}(\vec{r}_1) = 1, L^{i_2}(\vec{r}_2) = 1\right\} \tag{3}$$

Here $P_{i_1 i_2}(\vec{r}_2 - \vec{r}_1)$ is the probability of the event $\vec{r}$ with vector $\vec{r}_1$ in phase i_1 and vector $\vec{r}_2$ in phase i_2. It should be noticed that in many cases, the media is anisotropic and it is inappropriate to simplify the vector to a scalar parameter.

Fig. 2 illustrates the correlation function $P_{11}(r)$ of a heterogeneous material whose micrograph is presented in the inlet. The porosity in the micrograph is 0.5. When r$\diamondsuit$0, P$_{11}$(r)$\diamondsuit$ $v_1 = 0.5$. When r$\diamondsuit\infty$, P$_{11}$(r)$\diamondsuit$ $v_1^2 = 0.25 v_1^2 = 0.25$. The limiting function $v_1^2 = 0.25 v_1^2 = 0.25$ is also shown as a horizontal line in Figure 2 to illustrate the regression.

The most popularly used formula to represent the distribution function is an exponential function proposed by Corson (1974).

$$P_{ij}(r) = \begin{cases} v_i v_j - v_i v_j \exp\left(-c_{ij} r^{n_{ij}}\right) & i \neq j \\ v_i^2 + v_i\left(1 - v_i\right) \exp\left(-c_{ij} r^{n_{ij}}\right) & i = j \end{cases} \tag{4}$$

For a two-phase composite (including porous materials), i and j correspond to phases 1 and 2. The constants c_{ij} and n_{ij} are microstructure parameters obtained by fitting the real correlation curve. This relationship has been shown to be appropriate for random isotropic microstructures.

For anisotropic case, the direction of vector r should be taken into consideration. Saheli and Garmestani (2004) introduced a simplified form of an anisotropic two-point correlation function and used it for an axially symmetric sample. In that study, the empirical coefficient c_{ij}, a scaling parameter representing the correlation distance, is reformulated by a Fourier expansion. Tasking into account only the first order term:

$$c_{ij}(\theta, A) = c_{ij}^0 \left(1 + (1 - A)\sin\theta\right), \tag{5}$$

where A is a material parameter that represents the degree of anisotropy in a microstructure such that $A = 1$ corresponds to an isotropic microstructure, and c_{ij}^0 is the reference empirical coefficient.

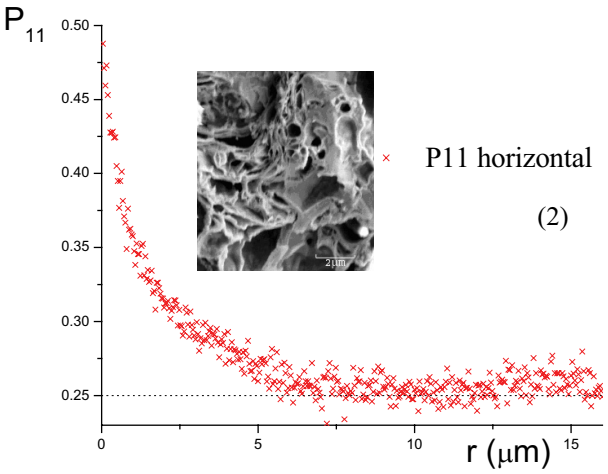

Figure 2 : The two-point correlation function P_{11} of the sample with inlet micrograph of LSM with porosity 0.5. Black dash line is $P_{11} = v_1^2 = 0.25$, where P_{11} is supposed to regress to.

In this study, for an anisotropic heterogeneous sample, a three dimensional form of the correlation function is proposed as below:

$$P_{ij}\left(\vec{r}(r,\theta,\phi)\right) = \begin{cases} v_i v_j - v_i v_j \exp\left(-c_{ij}(\theta,\phi)r\right) & i \neq j \\ v_i^2 + v_i\left(1-v_i\right)\exp\left(-c_{ij}(\theta,\phi)r\right) & i = j \end{cases} \tag{6}$$

We will use this formula in the next section to represent the microstructure of heterogeneous media.

3 Prediction of Properties

3.1 Prediction of Elastic Properties using Statistical Mechanics Model

Statistical continuum mechanics theory has been applied to a two-phase isotropic composite and polycrystalline materials for the prediction of elastic properties [Garmestani and Lin (2000, 2001); Beran, Mason, Adams and Olsen (1996)]. The work was extended to anisotropic composites by Saheli and Garmestani (2004). In this section, a brief overview on the use of the statistical continuum mechanics theory to calculate the elastic properties of composites will be shown.

The equilibrium equation and constitutive relationship are as follows:

$$\begin{aligned} &\sigma_{ij,j} = 0 \\ &\sigma_{ij}(x) = c_{ijkl}(x)\varepsilon_{kl}(x) \end{aligned}, \tag{7}$$

where $\sigma_{ij}(x), c_{ijkl}(x)$, and $\varepsilon_{kl}(x)$ are the local variables. Treating the heterogeneous material as a homogenous one, the effective elastic constants can be defined as:

$$\left\langle \sigma_{ij} \right\rangle = C_{ijkl}\left\langle \varepsilon_{kl} \right\rangle, \tag{8}$$

where ¡h¿ is called the ensemble average of property "h(x)" over the whole volume [Kroner 1972] and is defined by:

$$\langle h \rangle = \langle h(x) \rangle = \frac{1}{V}\int_V h(x)dV \tag{9}$$

Therefore assuming ergodicity, the local components can be defined as a summation of the ensemble average and the field fluctuation (as an example: $c(x) = \langle c \rangle + \tilde{c}(x)$)

The effective elastic constants can be calculated as (for details see Garmestani, et. al. (1999, 2000)):

$$C_{ijkl} = \left\langle c_{ijkl} \right\rangle + \left\langle \tilde{c}^{(}_{ijmn}x)a_{mnkl}(x) \right\rangle, \tag{10}$$

where a_{mnkl} is a fourth rank tensor defined to represent heterogeneity in strain field.

In Eq.(11), the second term is evaluated by [Saheli and Garmestani (2004)]:

$$\begin{aligned} &\left\langle \tilde{c}^{(}_{ijku}x)a^{(}_{kurs}x') \right\rangle \\ &= \int_V \partial\left[K_{kpu}(x,x')\left\langle \tilde{c}^{(}_{ijku}x)\tilde{c}^{(}_{pmrs}x') \right\rangle\right] \Big/ \partial x'_m dX' \\ &- \int_V K_{kpum}(x,x')\left\langle \tilde{c}^{(}_{ijku}x)\tilde{c}^{(}_{pmrs}x') \right\rangle dX' \end{aligned} \tag{11}$$

where $x$and x' are two different positions in the media, and dX′ is the volume integral on the volume element around position x′. In Eq. (11) $K_{kpu}$and$K_{kpum}$are respectively the first and second derivative of the Green's function and has been generally defined by Bacon (1979) for anisotropic composites as follows:

$$G_{ij,s}\left(x-x'\right) = \frac{1}{8\pi^2\left|x-x'\right|^3} \times \oint_{|z|=1}\left[T_s(zz)^{-1}_{ij} - z_s F_{ij}\right]dS$$

$$G_{ij,sr}\left(x-x'\right)=\frac{1}{8\pi^2\left|x-x'\right|^3}\times\oint_{|z|=1}\left[2T_sT_r\left(zz\right)_{ij}^{-1}-2\left(z_sT_r+z_rT_s\right)F_{ij}+z_sz_rE_{ij}\right]dS, \tag{12}$$

where$T_r$and $T_s$are the components of the unit vector that connects each two points in the sphere (the frame work for integration), and $(zz)_{ij}$and $(zz)_{ij}^{-1}$are the second rank tensor and its inverse. It is defined by:

$$(zz)_{ij}=C_{imkj}z_mz_k, \tag{13}$$

$\langle\tilde{c},\tilde{c}\rangle$is the two-point correlation function and for the case of composites may be derived as:

$$\left\langle\tilde{c}_{ijku}\left(x\right)\tilde{c}_{pmrs}\left(x'\right)\right\rangle=\tilde{c}^1_{ijku}\tilde{c}^1_{pmrs}p_{11}+\tilde{c}^1_{ijku}\tilde{c}^2_{pmrs}p_{12}+\tilde{c}^2_{ijku}\tilde{c}^1_{pmrs}p_{21}+\tilde{c}^2_{ijku}\tilde{c}^2_{pmrs}p_{22}, \tag{14}$$

where, c^1, $c^2$are the local elastic moduli for the two individual phases.

Knowing the correlation term and the Green's function, Eq. (11) can be estimated. As it's shown in Table (1), the limiting values of probabilities P_{11} (or P_{11}) are $v_1\left(v_2\right)$ and $v_1^2\left(v_2^2\right)$. In previous work [Saheli and Garmestani (2005)], it was shown that the first integral in Eq. (11) includes these limiting values. It was proved numerically and analytically that the first term is just the contribution of one-point probabilities whereas the second integral includes the information of two-point probabilities. Therefore the morphology of the microstructure has been contributed in the calculation of effective elastic properties. (For more details refer to Saheli and Garmestani, (2005))

Table 1 : Two-point Probability Functions in two phases composite under extreme condition of vector length.

	P_{11}	P_{12}	P_{21}	P_{22}
$x-x'\to 0$	V_1	0	0	V_1
$x-x'\to\infty$	V_1^2	$V_1\ V_2$	$V_1\ V_2$	V_2^2

Therefore, calculating the second integral in Eq. (11) and knowing the average values, the elastic moduli of the heterogeneous media can be estimated. For this purpose, the calculation has been done on a sphere. The sphere has been divided into $n_r\times n_\theta\times n_\phi$sections for performing the numerical evaluation. Measuring the two-point probability, the two integrals in Eq. (11) have been calculated and summed with the average value.

3.2 Prediction of Electrical Conductivity using Statistical Continuum Model

We assume that the heterogeneous media is composed of n constituents with different conductivities, σ^i, *(i=1...n)* and partitions v^i. The size of the inhomogeneity is significantly larger than the electron free path. Then the local current density j and local field E at any arbitrary point x satisfy the linear relationship such that:

$$j_i(x)=\sigma_{ij}(x)E_k(x) \tag{15}$$

in which $[j_i]$ is current and $[E_k]$ is field. This equation has a broad application. In the case of electric field, $[j_i]$ is current density; $[E_k]$ is electric field and $[\sigma_{ij}]$ is electric conductivity. In the case of magnetic field, $[j_i]$ is magnetic induction; $[E_k]$ is magnetic field and $[\sigma_{ij}]$ is magnetic permeability. In the case of heat transfer, $[j_i]$ is heat flux; $[E_k]$ is temperature gradient and $[\sigma_{ij}]$ is thermal conductivity. Similar equations can also be written to describe piezoelectric effect, Hall effect, dielectric permittivity and so on. The methodology developed here is applied to electrical conductivity prediction.

Effective conductivity σ_{eff} in the heterogeneous media is defined by the equation:

$$\langle J(x)\rangle=\sigma_{eff}\langle E(x)\rangle \tag{16}$$

Symbol ¡...¿ denotes the ensemble average that was defined in Eq.(9). The detailed procedure to obtain σ_{eff} is explained in the following. To define the relationship between the localized conductivity $\sigma(x)$ and the ensemble average of the conductivity, ¡σ¿, we introduce polarized conductivity $\tilde{\sigma}(x)$ such that:

$$\sigma(x)=\langle\sigma\rangle+\tilde{\sigma}(x) \tag{17}$$

If we define the polarized field P(x) as:

$$P(x)=\tilde{\sigma}(x)E(x) \tag{18}$$

then we have:

$$J(x)=\langle\sigma\rangle E(x)+P(x) \tag{19}$$

Since the current is divergence free:

$$\nabla\cdot J(x)=0=\langle\sigma\rangle\nabla\cdot E(x)+\nabla\cdot P(x) \tag{20}$$

Define a potential field φ such that:

$$E=-\nabla\varphi \tag{21}$$

Substitute Eq. (21) back to Eq. (20)

$$\langle\sigma\rangle \nabla\cdot(\nabla\varphi) = \nabla\cdot P(x) \tag{22}$$

Eq. (22) is a set of Partial Differential Equations that can be solved using a number of techniques. Using Green's function, the solution of Eq. (22) is given as:

$$\varphi(x) = \varphi_0(x) - \int dx'\nabla g(x,x')P(x') \tag{23}$$

$$g(x,x') = \frac{1}{4\pi\sigma_0}\frac{1}{x-x'} \tag{24}$$

To obtain the field E, Eq. (23) is differentiated:

$$E(x) = E_0 + \int dx' G(x-x')P(x') \tag{25}$$

The solution to the Green's function *G(x-x′)* is derived elsewhere [Torquato (2002)] but here we describe a numerical routine to perform the integration over the Green's function for an ensemble of aggregates in a heterogeneous medium. Because of the existence of a singular point in the integral at *x=x′*, a spherical region around the singular point has to be excluded. Using integration by parts and divergence theorem, the Green's function *G(x-x′)* is expressed as [Torquato (2002)]:

$$G(x-x') = -D\delta(x-x') + H(x-x') \tag{26}$$

where $D = \frac{1}{3\sigma_0}I$ and $H = \frac{1}{4\pi\sigma_0}\frac{3\hat{n}\hat{n}-I}{r^3}$.
Here I is the second order identity tensor and $\hat{n}$ is the unit vector for *x-x′*.
Substitute Eq. (18) for the definition of the polarized field back into Eq.(25):

$$E(x) = E_0 + \int dx' G(x-x') * \tilde{\sigma}(x')E(x') \tag{27}$$

Using Taylor series expansion, and taking into account only the first-order correction, we have:

$$E(x) = E_0 + \int dx' G(x-x') * \tilde{\sigma}(E_0, h(x'))E_0 \tag{28}$$

The average field for state h can be calculated from the above equation:

$$\langle E(x)\rangle_h = E_0 + \int dx' G(x-x') * \left\langle\tilde{\sigma}(E_0, h(x'))\right\rangle_h E_0 \tag{29}$$

The correlation function $\langle\tilde{\sigma}(E_0, h(x'))\rangle_h$ can be described in terms of the conditional two-point probability density function of state, h,

$$\left\langle\tilde{\sigma}(E_0, h(x'))\right\rangle_h = \int f\left(r' \in h(r') \,|r \in h\right)\tilde{\sigma}(E_0, h(x'))dh(r') \tag{30}$$

where conditional two-point correlation function $f(r' \in h(r') \,|r \in h)$ is defined as the probability of occurrence of *r′* at state *h(r′)* given that *r* belongs to state *h*:

$$f\left(r' \in h_j \,|r \in h_i\right) = P_{ij}/v_i \tag{31}$$

The corresponding two point probability function $P_{ij}(r,r')$ can be represented as shown before in Eq.(6). After the statistical localized field, $\langle E(x)\rangle_h$, is obtained, the corresponding statistical localized current density, $\langle j(x)\rangle_h$, is calculated from Ohm's Law:

$$\langle j(x)\rangle_h = \sigma_h \langle E(x)\rangle_h \tag{32}$$

Since no assumption is used on representing the statistical distribution of components in the heterogeneous media, the application of this statistical continuum model on the prediction of conductivity can cover a broad range of materials systems. For example, the formulation can be applied in a multi-phase composite framework assuming that the two phases are isotropic. Also the model can equivalently work in a porous medium where void is considered as a phase. The third example is polycrystalline materials that can be taken as an n-phase composite where each grain is considered as a different phase distinguished by its orientation.

4 Application of Multiscale Model in Materials Design of Fuel Cell Electrodes

In this section, multiscale model based on statistical and continuum mechanics is applied in microstructure sensitive design to guide the microstructure optimization in electrodes. Various processes have been employed in the fabrication of electrodes. To name a few, there are screen printing, tape casting and chemical vapor deposition. These fabrication methods are either time consuming or expensive. Plasma spraying is fast and inexpensive, but the deposit layer is thin. In our laboratory

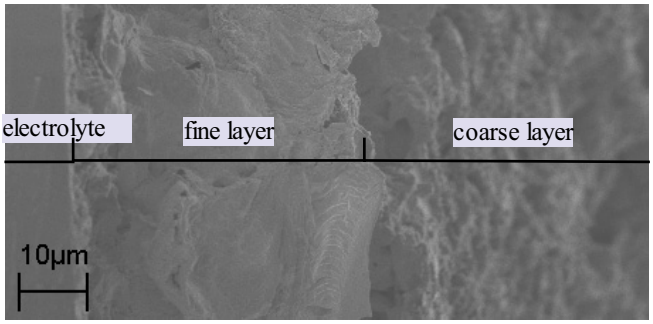

(a)

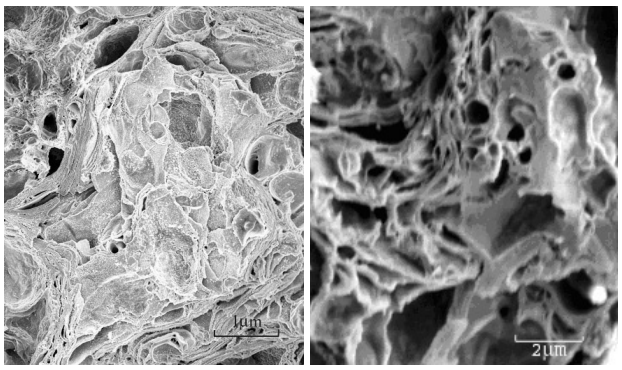

(b) (c)

Figure 3 : (a) Micrograph of double layered LSM deposited on YSZ at a cross section view. (b) Magnified micrograph of fine layer of LSM. (c) Magnified micrograph of coarse layer of LSM.

spray pyrolysis is utilized to fabricate the cathode materials. Using this method, deposit rate is fast. Cathode layer is thick and uniform. It is a good candidate in large scale fabrication process. By adjusting the process parameters, such solvent, droplet size, deposition temperature, pressure, the distance between the spray nozzle and the substrate, the microstructure of fabricated cathode can be controlled. For example, a fine layer can be achieved when using small droplet size. Increasing the droplet size, the embedded particles become larger and the microstructure becomes coarse. By changing the droplet size gradually during fabrication, a gradient or multilayer microstructure can be obtained.

Figure 3 illustrates the cross view microstructure of gradient LSM cathode deposited on YSZ electrolyte. Fig. 3(a) shows the three sections from left to right: electrolyte, fine layer of LSM cathode and coarse layer of LSM. A fine layer of LSM was fabricated using dyglime/bet diketontes followed by a coarse layer using the aqueous solution. Fig. 3(b) is a magnified micrograph of LSM inner layer closer to the electrolyte. The pores are small and particles are fine. This kind of microstructure is supposed to have better electrochemical activity. Fig. 3(c) is a magnified micrograph of LSM outer layer. The pores are large and particles are coarse. It is supposed to have better transport properties while offering the required mechanical support.

To characterize the microstructure in cathodes, modified Corson's equation presented in Section 2 is applied. Figure 4 gives the evolution of probability P_{11} with vector length in coarse layer at different vector orientations. Black square points are from horizontal vectors thrown in the coarse layer. Red triangle points are from vertical direction. Black solid line and red dash line are the corresponding fitting curve according to Eq. (6) for horizontal and vertical cases respectively. It is difficult to figure out the anisotropy from the micrograph by direct observation. However, the correlation function curves clearly show the existence of anisotropy in the sample. Our prediction of conductivity in a later section also reveals differences in effective conductivity between the horizontal and vertical directions.

The fit curves in Fig. 4 give the correlation parameter c_{ij} for coarse layer at horizontal and vertical directions. Combined with other correlation parameters at other directions, the evolution of parameter c_{ij} with direction (represented by $sin\theta$) is shown in Fig. 5. A Linear fit of these points gives two correlation parameters for the coarse layer: $c_{ij}^0 = 0.67$ and $A = 0.45$. A is an indictor of anisotropy. The corresponding value in fine layer is 0.77, shown in Table 1. As discussed earlier in Section 2, A is in the range of 0 and 1 and smaller A indicates higher anisotropy. By this definition, it will be expected that the coarse microstructure with smaller A shows more anisotropy in the effective properties. This will be proved later in the prediction of properties along different directions.

Table 2 : Microstructure parameter and predicted properties in two layers of LSM with porosity of 0.5.

Layer	Fine	Coarse
A	0.77	0.45
Conductivity (horizontal) (S/cm)	105	113
Conductivity (vertical) (S/cm)	104	101
Elastic Modulus (horizontal) (GPa)	42.2	45.2
Elastic Modulus (vertical) (GPa)	42.7	37.6

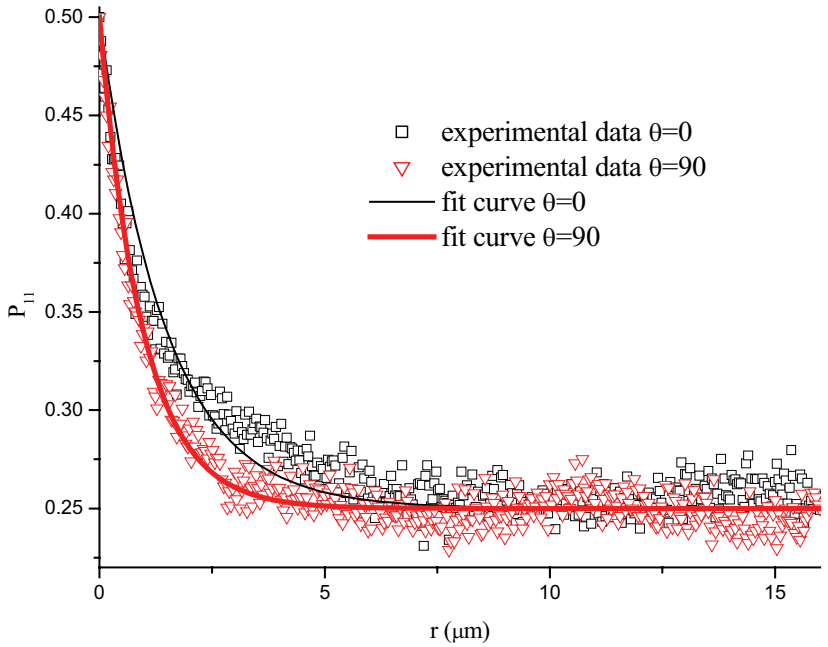

Figure 4 : The two-point correlation function P_{11} of the coarse layer of LSM along horizontal and vertical directions respectively. Curves are fit according to modified Corson's function.

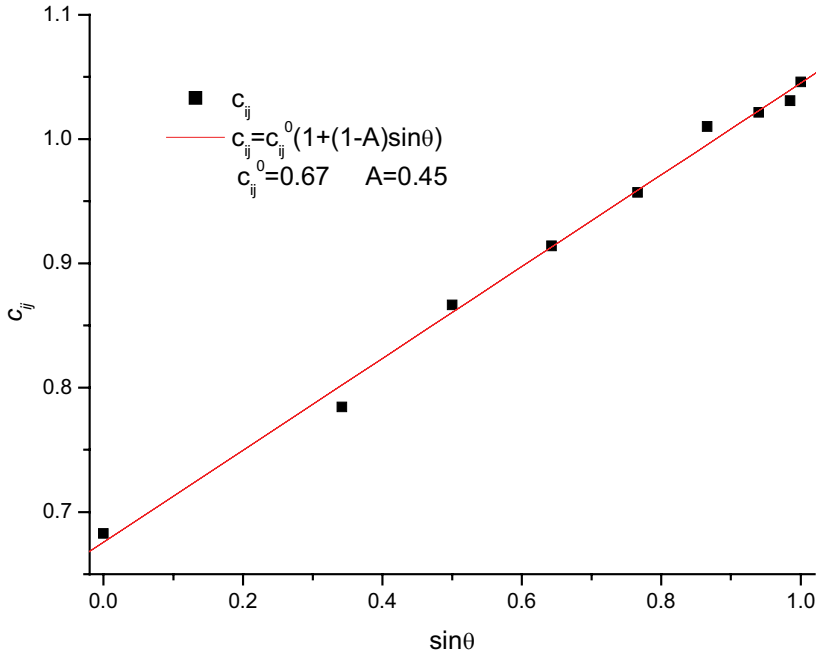

Figure 5 : Correlation function parameter c_{ij} at different angle θ. Fit curve gives parameters c_{ij}^0 and A in modified Corson's function.

The electrical and mechanical properties of different layers in the electrode with porosity of 50% from the statistical continuum model are also shown in Table 2. Yasuda and Hishinuma (1996) reported the electrical conductivity in LSM of 210S/cm at the temperature of 1273K. Young's modulus of 120Gpa in LSM was reported by

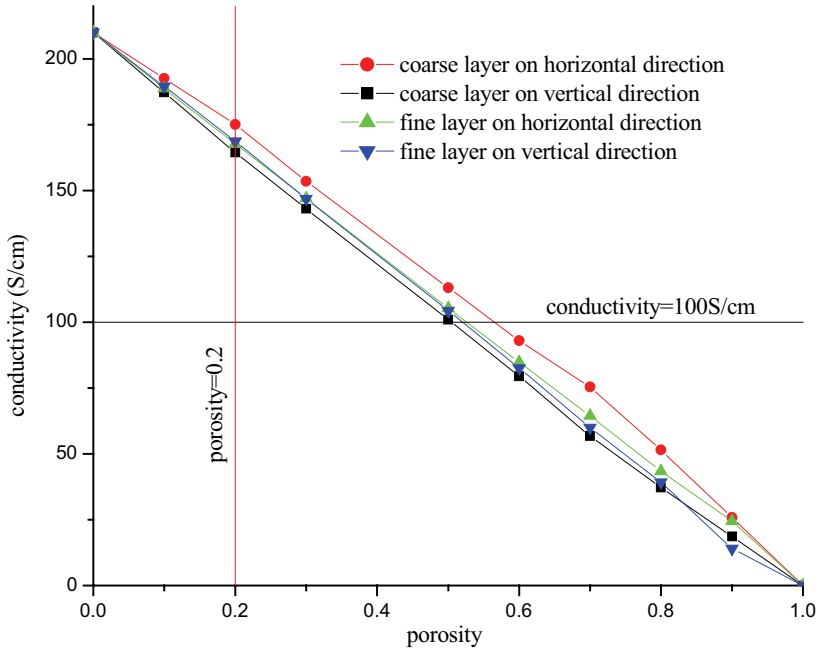

Figure 6 : Prediction of normalized conductivity of two layers in the LSM cathode along two directions at different porosity using multiscale model.

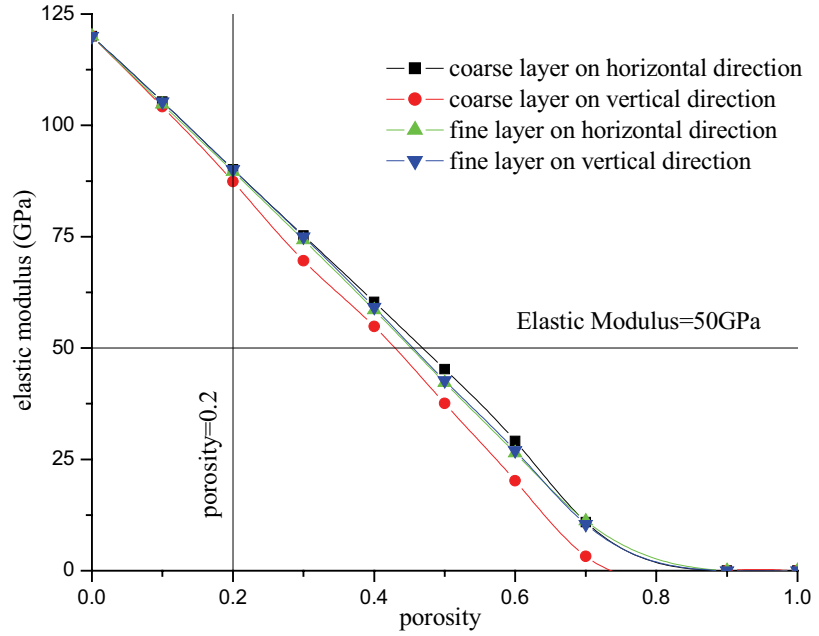

Figure 7 : Prediction of normalized elastic modulus of two layers in LSM cathodes along two directions at different porosity using multiscale model

Meixner and Cutler (2002). These measured values were used for pure LSM in prediction. The difference of conductivities along vertical and horizontal directions in coarse layer is 12S/cm. On the other hand, difference in fine layer is only 1S/cm, more than 10 times lower than that in coarse layer. This is comparable with the pre-

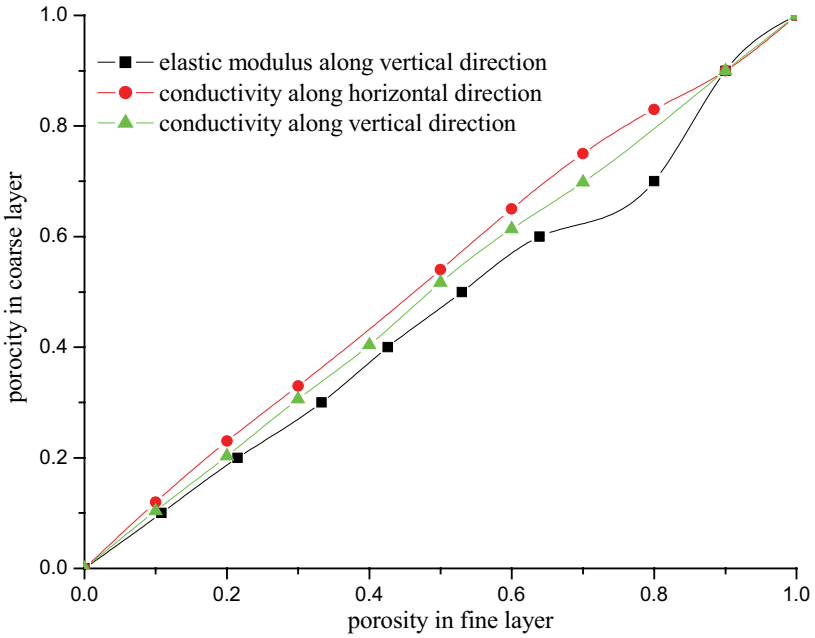

Figure 8 : Corresponding volume fractions of LSM in two layers with identical properties

diction results of mechanical properties. The difference of normalized elastic modulus along directions in coarse layer is 7.5GPa. In contrast, difference in fine layer is only 0.5GPa, also more than 10 times lower than that in coarse layer. The anisotropy reflected from the predicted properties corresponds to the differences in the correlation parameters: fine layer in this sample is isotropic while coarse layer more anisotropic. Particles in the coarse layer are somehow oriented along horizontal direction although it is not obvious from the micrographs.

Microstructures with similar morphology but different porosity were generated by computers. From the simulated micrographs, the evolution of conductivities in electrodes with porosity was predicted using the multiscale model. The results are presented in Fig. 6. It is evident that the coarse layer is more anisotropic since the differences in the values of conductivities in different directions are larger. Conductivity in coarse layer along horizontal direction is highest, followed by conductivity in fine layer along horizontal direction, conductivity in fine layer along vertical direction and coarse layer along vertical direction in sequence. Conductivity curves along two directions in fine layer are so close that it is difficult to distinguish them. This confirms the isotropy shown from the statistical correlation analysis. Conductivity curves in coarse layer reflect the anisotropy revealed by A of 0.45.

Anisotropy is also captured in the prediction of mechanical properties of the electrodes from the model, as shown in Fig. 7. Elastic moduli in fine layer along two directions are indistinguishable; however they are significantly different for coarse layer. The inner two curves represent the elastic modulus for fine layer in horizontal direction and vertical direction. The outer two curves describe elastic properties in coarse layer.

Furthermore, prediction results of electrical and mechanical properties of electrodes can be used to guide the design of microstructure. For example, the electrode is required to have porosity higher than 20% for necessary permissibility and conductivity (along horizontal direction) higher than 100S/cm. From Fig. 6, the material designer can obtain the microstructure satisfying the requirements: porosity in coarse layer from 0.2 to 0.57 while porosity in the fine layer from 0.2 to 0.53. In the other case, the electrode is required to have a porosity higher than 0.2 and elastic modulus (along horizontal direction) higher than 50GPa. From Fig. 7, the optimal porosity satisfying the requirement is: 0.2 to 0.47 in coarse layer and 0.2 to 0.45 in fine layer. If both criteria of mechanical and electrical properties have to be considered, the porosities should be: 0.2 to 0.47 in coarse layer and 0.2 to 0.45 in fine layer.

As demonstrated above, MSD provides the range of microstructures which satisfy the required properties. Another application of MSD in materials design for fuel cell electrodes is on properties compatibility. All components of fuel cells, including electrodes, electrolytes and interconnects are required to have compatibility on chemical activity, thermal expansion and conductivity. For a multi-layer electrode, similar compatibility among different layers should also be considered. If the components of fuel cells are assembled in horizontal direction, as shown in Fig. 3, then the conductivity along horizontal direction should be compatible, at least comparable, to avoid bottleneck. Corresponding volume fractions of electrodes in coarse and fine layers with identical properties are illustrated in Fig. 8. For example, the fine layer with porosity of 0.3 has the same conductivity along horizontal direction as the coarse layer with porosity of 0.33. In electrode support systems, the mechanical property compatibility is also important. Fig. 8 shows that the fine layer with porosity of 0.3 has the same elastic modulus along horizontal direction as the coarse layer with porosity of 0.31. On the other hand, the fine layer with porosity 0.3 corresponds to coarse layer with porosity 0.27 when the elastic modulus along vertical direction is taken as criteria.

5 Conclusions

Effective electrical and mechanical properties in anisotropic heterogeneous media were predicted by a multiscale model based on statistical continuum mechanics models. In this study a two-point correlation function is used to characterize the microstructure that takes into account continuity, morphology, shape or distribution of the constituents. Embedding this model into a microstructure sensitive design framework, microstructure optimization was studied in materials design of fuel cell electrodes. Examples were given to demonstrate how MSD located microstructures satisfying the property requirement and compatibility. These solutions can be utilized to guide fabrication optimization. By adjusting fabrication parameters directed by MSD, the microstructure can be tailored to maximize performance.

Acknowledgement: The authors would like to acknowledge the support provided by Battelle-Pacific Northwest National Lab with grant #1806C44 and DOE grant #DE-FC07- 06ID14750.

References

Adams BL, Henrie A, Henrie B, Lyon M, Kalidindi SR, Garmestani H. (2001): Microstructure-sensitive design of a compliant beam. *J Mech Phys Solids*, vol. 49, pp. 1639-1663.

Adams BL, Lyon M, Henrie B. (2004): Microstructure by design: linear problems in elastic-plastic design. *Int J Plast*, vol. 20, pp. 1577-1602.

Bacon, D.J., Barnett, D.M., and Scattergood, R.O. (1978): Anisotropic Continuum theory of lattice defects, *Progress in Materials Science*, vol. 23, pp. 51-262.

Beran, M. J. (1968): *Statistical continuum theories.* Interscience Publishers, NewYork.

Beran, M.J., Mason, T.A., Adams, B.L., and Olsen, T. (1996): Bounding elastic constants of an orthortropic polycrystal using measurements of the Microstructure, *J Mech Phys Solids*, vol. 44, pp. 1543-1563.

Castaneda, P. (1991): The effective mechanical properties of nonlinear isotropic composites. *J Mech Phys Solids*, vol. 39, pp. 45-71.

Corson, P.B. (1974): Correlation functions for predicting properties of heterogeneous materials. I. Experimental measurement of spatial correlation functions in multiphase solids. *J Appl Phys*, vol. 45, pp. 3159-3164.

Garmestani H., Lin S. (2000): Statistical continuum mechanics analysis of an elastic two isotropic phase composite material", *J Composites: Part B*, vol. 31, pp. 39-46.

Garmestani H., Lin S., Adams B., Ahzi S. (2001): Statistical continuum theory for texture evolution of polycrystals. *J Mech Phys Solids*, vol. 49, pp. 589-607.

Gavarri J.R., Tortet L. and Musso J. (1999): Transport properties and percolation in two-phase composites. *Solid State Ionics*, vol. 117, pp. 75-85.

Greengard, L. and Moura, M. (1994): On the numerical evaluation of the electrostatic fields in composite materials. *Acta Numerica*, Cambridge University Press, Cambridge, pp.379-410.

Grove, W.R. (1839): On Voltaic Series and the Combination of Gases by Platinum. *Philos Mag*, vol. 14, pp. 127

Kalidindi SR, Houskamp JR, Lyon M., Adams BL. (2004): Microstructure sensitive design of an orthotropic plate subjected to tensile load. Gradient based non-linear

microstructure design. *Int J Plast*, vol. 20, pp. 1561-1575.

Kroner, E. (1972): *Statistical continuum mechanics*. Springer Verlag, Wien., NY.

Kröner, E. (1977): Bounds for effective elastic moduli of disordered materials. *J. Mech. Phys.Solids*,vol.25, pp 137-55.

Li, D.S, Garmestani, H., Schoenfeld S.E. (2003): Evolution of crystal orientation distribution coefficients during plastic deformation. *Scripta Mater*, vol. 49, pp. 867-872.

Li, D.S., Garmestani, H, B.L. Adams. (2005): A processing path model for texture evolution in cubic-orthortropic polycrystalline system. *Int J Plast*, vol. 21, pp. 1591-1617.

Lin S., Adams B. L., Garmestani H. (1998): Statistical continuum theory for inelastic behavior of two-phase medium. *Int J Plast*, vol. 14 pp. 719-731

Lin S., Garmestani H., Adams B.L. (2000): The evolution of probability functions in an inelastically deforming two-phase medium. *Int J Solids Struct*, vol. 37, pp. 423

Meixner, D.L.; Cutler, R.A. (2002): Sintering and mechanical characterization of lanthanum strontium manganite. *Solid State Ionics*, vol. 146, pp. 273-284.

Michel, J.C., Moulienec, H. and Suquet, P. (2001): A computational scheme for linear and non-linear composites with arbitrary phase contrast. *Int J Numer Meth Eng*, vol. 52, pp. 139-160.

Rodin, G.J. (1993): The overall response of materials containing spherical inhomogeneities. *Int J Solids Struct*, vol.30, pp. 1849-1863.

Saheli, G., Garmestani H., and Adams B.L. (2004): Microstructure design of a two phase composite using two-point correlation functions. *J Comp-Aided Mater Design*, vol. 11, pp. 103.

Saheli, G., Garmestani, H., and Gokhale, A. (2005): Homogenization relations for elastic properties of two-phase composites using two-point statistical functions. Submitted to the *Journal of Physics and Mechanics of Solids*.

Shen, S.P.; Atluri, S.N. (2004): Computational Nano-mechanics and Multi-scale Simulation, *CMC: Computers, Materials, & Continua*, Vol. 1, pp. 59-90

Torquato, S. (2002): *Random Heterogeneous Materials: Microstructure and Macroscopic Properties*, Springer-Verlag, New York.

Walpole, L.J. (1981): Elastic behavior of composite materials: Theoretical foundations. *Adv Appl Mech* Vol. 21, pp. 169-242

Williams, M.C., Strakey, J.P; Sinhal, S.C. (2004): U.S. distributed generation fuel cell program. *J Power Sources*, vol. 131, pp. 79-85.

Willis, J.R. (1981): Variational and related methods for the overall properties of composites. *Adv Appl Mech* Vol. 21, pp. 1-78.

Yasuda, I.; Hishinuma, M. (1996): Electrical conductivity and chemical diffusion coefficients of strontium-doped lanthanum manganite. *J Solid State Chem*, vol. 123, pp. 382-390.

Zhu, W.Z.; Deevi, S.C. (2003). A review on the status of anode materials for solid oxide fuel cells. *Mater Sci Eng*, vol. A362, pp. 228-239.